Changes of sewage sludge digestate-derived biochar properties after chemical treatments and influence on As(III and V) and Cd(II) sorption

Suchanya Wongrod, Stéphane Simon, Eric D. van Hullebusch, Piet Lens, Gilles Guibaud

Changes of sewage sludge digestate-derived biochar properties after chemical treatments and the influence on As(III and V) and Cd(II) sorption

Suchanya Wongrod[a,b,c], Stéphane Simon[b,*], Eric D. van Hullebusch[a,c,d], Piet N.L. Lens[c], Gilles Guibaud[b]

[a] Université Paris-Est, Laboratoire Géomatériaux et Environnement (EA 4508), UPEM, 77454, Marne-la-Vallée, France

[b] Université de Limoges, PEIRENE, Equipe Développement d′indicateurs ou prévision de la qualité des eaux, URA IRSTEA, 123 avenue Albert Thomas, 87060 Limoges, France

[c] UNESCO-IHE Institute for Water Education, P.O. Box 3015, 2601 DA Delft, The Netherlands

[d] Institut de Physique du Globe de Paris, Sorbonne Paris Cité, Université Paris Diderot, UMR 7154, CNRS, F-75005 Paris, France

[*] Corresponding author. Université de Limoges, PEIRENE, Equipe Développement d′indicateurs ou prévision de la qualité des eaux, URA IRSTEA, 123 avenue Albert Thomas, 87060 Limoges, France
Email: stephane.simon@unilim.fr

Abstract

This work seeks to extend the knowledge on the effect of chemical treatments of sewage sludge digestate (SSD)-derived biochar for As(III and V) and Cd(II) sorption ability using potassium hydroxide (KOH) or hydrogen peroxide (H_2O_2). Results showed the increases of pH of point of zero charge, the Brunauer-Emmett-Teller (BET) surface area and cation exchange capacity (CEC) after chemical treatments of biochar. The sorption ability was enhanced from 1.6 µmol g^{-1} (As(V)) and 16.1 µmol g^{-1} (Cd(II)) on raw biochar to 8.5 µmol g^{-1} (As(V)) and 318.5 µmol g^{-1} (Cd(II)) on KOH-modified biochar. Furthermore, arsenic redox distribution showed a large oxidation (70%) of As(III) to As(V) in KOH-biochar with batch washing, while a partial oxidation (7%) was observed in KOH-biochar with batch and subsequently column washing. The washing procedures after KOH treatment play an important role on arsenic sorption, due to the release of phosphate (PO_4^{3-}) as well as organic matter from the biochar that may subsequently lead to the oxidation of As(III) to As(V). Our findings highlight the potential influence of biochar on the redox transformation of As(III) to As(V) and therefore require a careful assessment while investigating the fate of As in aquatic environments.

Keywords: Sewage sludge digestate derived biochar, chemical activation, As(III), As(V), Cd(II), biochar washing

1. Introduction

Arsenic (As) and cadmium (Cd) contamination in water creates a pressing toxicity towards aquatic organisms. Arsenic is mostly present as two inorganic species, arsenite (As(III)) and arsenate (As(V)), whereas a divalent cadmium ion (Cd(II)) dominantly prevails in water. Due to the toxicity of As and Cd, numerous treatments have been dedicated to removing these elements from polluted water. Among them, sorption is a cost-effective and simple treatment for metal(loid) removal from water (Ding et al., 2016; Ofomaja et al., 2014; Peng et al., 2018; Wang et al., 2016; Zhou et al., 2017). In recent years, biochar, a black solid char obtained from pyrolysis (> 250 °C) of biomass under oxygen-limiting conditions (Ahmad et al., 2014), has been considered as a potential alternative to activate charcoal in sorption treatments. Sewage sludge digestate (SSD) obtained from wastewater treatment plants is currently considered as a promising material to produce a low-cost biochar (Agrafioti et al., 2013; Rajapaksha et al., 2014; Yuan et al., 2015; Zielińska and Oleszczuk, 2015).

During the pyrolysis step of biochar preparation, the organic matter from biomass undergoes structural modifications such as oxidation and conversion of aliphatic forms to aromatic forms (Zama et al., 2017). The resulting biochar generally harbors negative and positives charges on its surface depending on the neighboring pH. Consequently, at circumneutral pH, where negative charges are predominant, it has been applied to sorb cationic metals like lead (Pb), zinc (Zn) and cadmium (Cd) from polluted water (Ding et al., 2016; Ho et al., 2017; Park et al., 2017; Wongrod et al., 2018). Unfortunately, the sorption ability of SSD biochar for metal(loid)s, particularly As oxyanions, is relatively low compared to activated carbon or paper mill sludge biochar (Table S1, supplementary information). Therefore, biochar modifications like physical activation and chemical treatment have been applied to improve its sorption ability (Li et al., 2017; Rajapaksha et al., 2016; Sizmur et al., 2017). Even though there are many studies on the adsorption capacity of raw and modified biochars (Liu et al., 2017; Zuo et al., 2017), an evaluation of the modification of the biochar properties is yet to be done. Indeed, the biochar surface properties are important parameters that influence the behavior of a sorbent to sorb anionic and cationic pollutants.

The present work aimed to study the consequences of chemical treatments of SSD biochar using KOH or H_2O_2 on its arsenic and cadmium sorption capacities. Batch experiments were performed to evaluate the sorption kinetics and capacity of raw and modified biochars for As(III, V) and Cd(II). Several surface properties, such as the pH of point of zero charge (pH_{PZC}), the cation exchange capacity (CEC) and the Brunauer-Emmett-Teller (BET) surface area were determined to access information on, respectively, the net surface charge, cation exchange capacity and available specific surface area of the SSD biochars. These parameters can be used to discuss the sorption characteristics of the biochar. The influence of chemical modifications of the biochar onto sorption of redox-sensitive elements was also investigated through the determination of arsenic redox transformation (*i.e.* As(III) and As(V)) during sorption experiments. Finally, the consequences of biochar washing on all these parameters were considered by comparing the results obtained with a KOH-modified biochar submitted either to only a batch washing or to a subsequent continuous column washing.

2. Materials and methods

2.1 Chemical reagents

Cadmium ($Cd(NO_3)_2.4H_2O$, 99% *w/w*, Merck), arsenate ($Na_2HAsO_4.7H_2O$, 98% *w/w*, Sigma-Aldrich) and arsenite ($AsNaO_2$, 98% *w/w*, Merck) were used to prepare 10 mM of Cd(II), As(V) and As(III) stock solutions, respectively. The ultrapure water (18.2 MΩ, MilliQ Gradient A10, Millipore SAS 67120, Molsheim, France) was used to wash biochars, as well as to prepare and dilute all solutions and samples.

2.2 Biochar preparation and chemical treatment

Pellets of domestic sewage sludge digestate (SSD) were obtained from a wastewater treatment plant (WWTP) located in Limoges, France (size: 285,000 equivalent population). The main treatment processes of the WWTP include activated sludges with anoxic treatment and addition of iron(III) chloride ($FeCl_3$) to, respectively, remove nitrogen(N) and phosphorus (P). Particularly, the SSD sample was collected in the storage tank after dewatering and drying processes.

The sample was heated at 350 °C for 15 min under slow pyrolysis technology to produce SSD biochar and more information was described in our previous work (Wongrod et al., 2018). The SSD biochar was chemically treated for 2 h with a 10% H_2O_2 solution (100 g: 1 l) or with 2 M KOH solution (100 g: 2.5 l) (Wongrod et al., 2018).

The raw and chemically-modified biochars were subsequently washed as follows: a triple batch washing in a row followed by a continuous column washing (Wongrod et al., 2018). These washing steps were performed to remove competitive ions (*e.g.* PO_4^{3-}, HCO_3^-/CO_3^{2-}, Ca^{2+} and Mg^{2+}) and organic matter released by the biochar during the chemical treatment. These released compounds can react with elements and thus interfere with the biochar-metal(loid) sorption system. In addition, clogging of the biochar pore sites by small particles can be eliminated through these washing steps. To determine if the washing procedure influence the metal(loid) sorption, a KOH-modified biochar was washed only with a batch procedure. The raw SSD biochar, its H_2O_2 and KOH-modified SSD biochar are denoted as, respectively, BSS, BH_2O_2 and BKOH. The KOH-modified biochar washed with only the batch procedure is labeled as $BKOH^{bat}$.

2.3 Biochar characterization

X-ray powder diffraction (XRD) and Fourier transform infrared spectroscopy (FTIR) of the SSD and its derived biochar were analyzed to observe the changes of, respectively, crystalline structures and surface functional groups after biochar production. The total amount of metal and metalloid in the SSD and its derived biochar was determined using acid digestion from the EPA Method 3050B (EPA, 1996). The details of the digestion procedures are described by Wongrod et al. (2018).

The pH (pH-meter LPH 330T, Tacussel, France) and electrical conductivity (EC) (CDM 210 conductivity-meter, Radiometer, Denmark) of the biochar were measured in water. The

surface area of biochar was measured using N_2 sorption by the Brunauer-Emmett-Teller (BET) method at 77 K (3Flex, Micromeritics, USA). Pretreatment of biochar was performed by drying at 105 °C for 5 h prior to the BET surface area (S_{BET}) analysis.

The pH of point of zero charge (pH_{PZC}) of the biochar was determined from zetametry by determining the zeta potential at different pH ranges (Mahmood et al., 2011). For the determination of the cation exchange capacity (CEC), 2 g of biochar (dry weight) were mixed with 40 ml of 0.05 N cobalt hexamine trichloride ($[Co(NH_3)_6]Cl_3$) solution (99% *w/w*, Sigma-Aldrich) in polypropylene tubes (Aran et al., 2008). The details of the biochar preparation for pH_{PZC} and CEC measurement are provided in the supplementary information.

2.4 Sorption experiments

In sorption kinetic experiments, 10 µM As(III), As(V) and Cd(II) were prepared separately from stock solutions of 1 mM As(III), As(V) and Cd(II) (as $AsNaO_2$, $NaHAsO_4.7H_2O$ and $Cd(NO_3)_2$, respectively). Raw and modified biochars (600 mg) were added to 150 ml of metal(loid) solution. The initial pH was adjusted to 5 using HNO_3 and NaOH. The solutions were agitated at (20 ± 2) °C at 180 rpm for 24 h using an orbital shaker (KS 501 digital, IKA^{TM}, USA). The sorption experiments were performed in duplicate. Samples of solution were collected over time. The total collected volume was less than 5% of the initial volume to prevent any alteration of the sorption equilibrium. Sampled solutions were filtered through Lab Logistics Group (LLG) cellulose acetate syringe filters (0.45 µm) and their As and Cd concentrations were determined by graphite furnace atomic absorption spectrometry (240Z, Agilent Technologies, USA) at λ 193.7 nm and λ 228.8 nm for As and Cd, respectively. The pseudo-first-order (PFO) and the pseudo-second-order (PSO) kinetics models were used to describe the experimental data. The intraparticle diffusion model was also studied to access information on the mechanism of the sorption processes (Zhao et al., 2015a).

Adsorption isotherms were performed with initial concentrations ranging from 10 to 300 µM for As(III, V) and from 10 to 4000 µM for Cd(II). After 24 h of agitation, the residual concentrations of As were determined by graphite furnace atomic absorption spectrometry as detailed previously, whereas the residual concentrations of Cd were determined by Microwave Plasma Atomic Emission Spectroscopy (MP-AES) (Agilent 4100, USA) at λ 228.8 nm. Two common adsorption isotherm models (Langmuir and Freundlich) were used to fit the experimental data. Arsenic speciation was determined by High-Performance Liquid Chromatography (HPLC) coupled to Atomic Fluorescence Spectrometry (AFS) with Hydride Generation (HG) (PS Analytical Millennium Excalibur, P S Analytical, UK). For the chromatographic conditions, a Hamilton PRP-X100 column was used with a phosphate buffer solution as the mobile phase at a rate of 1 ml min^{-1}. Detailed information can be found in Wan et al. (2014).

2.5 Statistical analysis

Results are reported as means ± standard deviation (n=3) unless otherwise stated. Uncertainties of sorption parameters were obtained by non-linear regression using Statistica

software (v6.1, StatSoft). The t-test with two-tailed distribution at a statistical significance level of $P \leq 0.01$ were used for data comparison.

3. Results and discussion

3.1 Influence of chemical treatment on biochar characteristics

The XRD analysis showed that quartz was present in both SSD and BSS with insignificant modification of the surface properties after biochar pyrolysis (Fig. S1). FTIR spectra demonstrated similar binding between atoms of both the SSD and BSS (Fig. S2). The absorbance peaks of hydroxyl (–OH) groups (3425 cm^{-1}), $–CH_3$ stretching of aliphatic groups (2924 cm^{-1}), C=C stretching vibrations (1600 cm^{-1}), and C–C skeleton and C–O stretching (1033cm^{-1}) were mainly detected on the SSD and BSS (Fig. S2). These functional groups can be involved in the sorption for metal(loid)s (Pituello et al., 2014).

The pH values of the suspensions of the raw and chemically-modified biochars are given in Table 1. The KOH treatment induced a change from 6.4 (± 0.1) for BSS to 8.4 (± 0.1) for BKOH and 10.1 (± 0.1) for $BKOH^{bat}$, whereas no significant difference ($P \leq 0.01$) was observed after H_2O_2 treatment (Table 1). Results also showed no significant changes of the electrical conductivity (EC) among each biochar suspension (*i.e.* BSS, BH_2O_2 and BKOH), except for $BKOH^{bat}$ where a 50-fold higher value (324 ± 2 µS cm^{-1}) was observed. The high EC value of $BKOH^{bat}$ is probably due to a significant release of weakly sorbed ions (*e.g.* PO_4^{3-}, HCO_3^-, CO_3^{2-}, Ca^{2+} and Mg^{2+}) from $BKOH^{bat}$ as previously reported by Wongrod et al. (2018). A previous study published by Yuan et al. (2015) is in agreement with our finding, as the authors have reported a very high EC of 7750 µS cm^{-1} in the sewage sludge biochar that was not washed with ultrapure water after pyrolysis (Table 1).

Fig. 1 shows the evolution of the zeta potential according to pH values for BSS, BH_2O_2, BKOH and $BKOH^{bat}$. The corresponding pH_{PZC} are given in Table 1. Results demonstrated similar pH_{PZC} values for both BSS (~2.7) and BH_2O_2 (~2.9) biochars, whereas a slightly higher value was obtained for BKOH (~3.4). Such limited variations of pH_{PZC} (2.7 – 3.4) are not prone to significantly modify the pH on the As and Cd sorption, except if the manipulations are performed at a pH lower than 5 (*i.e.* pH at sorption experiment, see section 2.4). In contrast, the more negative values of zeta potential observed for BH_2O_2 and $BKOH^{bat}$ (Fig. 1) could indicate higher amounts of negative charges at the surfaces of these two modified biochars, resulting in higher sorption capacities towards cationic metals.

The pH_{PZC} results showed that all biochars carried net negative charges at neutral pH (Fig. 1). At present, the pH_{PZC} of biochar has been rarely reported in the literature and there is a lack of information to understand its variability among different chemical treatments. However, our results are in agreement with a straw-derived biochar with a pH_{PZC} ~1.9 (Qiu et al., 2009) and a paper mill sludge with pH_{PZC} ranging from 4.0 – 6.0 (Guo et al., 2018).

The BET surface area (S_{BET}) of the raw and modified biochars is given in Table 1. A significant increase of the S_{BET} was observed for BH_2O_2 and BKOH, from 0.4 (± 0.1) to 5.7 (± 0.1) and 7.9 (± 0.1) $m^2\ g^{-1}$, respectively. This increasing S_{BET} is an indicator of higher porosity on the modified biochar and thus a growing chance for metal(loid)s to sorb onto the biochar surface (*e.g.* by complexation) (Mohan et al., 2014). Our findings are similar to those determined for

sewage sludge biochars (4.0 – 14.3 m^2 g^{-1}) (Agrafioti et al., 2013; Yuan et al., 2015) and pineapple-peel-derived biochars (0.7 – 2.1 m^2 g^{-1}) (Wang et al., 2016). Nevertheless, these values are still far lower than those reported for activated carbons (1215.0 – 1316.0 m^2 g^{-1}) (Gong et al., 2015).

The CEC values determined for the different biochars are presented in Table 1. Results showed a slight increase of CEC after treating the biochar with H_2O_2 from 1.9 (± 0.1) to 3.0 (± 0.1) $cmol^+$ kg^{-1}, whereas a significantly increase (6 times) after the KOH treatment ($P \leq 0.01$) was reported. This higher CEC of BKOH could induce an enhanced sorption ability towards cationic metals. Previously published data showed variable high ranges of the CEC of the biochars from 45.7 $cmol^+$ kg^{-1} to 483.4 $cmol^+$ kg^{-1} on wood and straw-based biochars, respectively (Ding et al., 2016; Jiang et al., 2014).

The variations in the S_{BET} and CEC after chemical treatments of the biochars suggest that H_2O_2 and KOH-modified biochars provided higher amounts of active pore sites, surface functional groups and exchangeable cations that could enhance the sorption of metallic elements on the biochar surface. For anion sorption, the increase of S_{BET} could influence the arsenic sorption capacity (Table 1).

Concerning the effect of the washing procedures after KOH treatment, the results showed significantly higher values of both pH and conductivity on $BKOH^{bat}$ than BKOH (Table 1), which were attributed to a release of ions such as PO_4^{3-} and HCO_3^{2-}/CO_3^{2-} from the biochar (Wongrod et al., 2018). As discussed previously (Wongrod et al., 2018), the insufficient batch washing after biochar modification led to the release of ions (*e.g.* PO_4^{3-}, HCO_3^{-}/CO_3^{2-}, Ca^{2+} and Mg^{2+}) and organic compounds from the biochar which interacted with metals and modified the sorption behavior. In the case of As(V), PO_4^{3-} is expected to be a strong competitor, reducing its sorption onto the biochar. The pH_{PZC}, S_{BET} and CEC values were also significantly affected by the uncomplete batch washing, resulting in an alteration of the biochar surface properties.

3.2 Effect of chemical treatment and washing on Cd(II) sorption

The results for the kinetic study of the Cd(II) sorption fitted better to the pseudo-second-order (PSO) (Fig. 2a) than intraparticle diffusion (Fig. 2b) models. All values for the kinetic model-fitting can be found in Table 2 and Table S2 (supplementary information). Results showed that the sorption of Cd(II) by all biochars were well-described by the PSO kinetic model (Table 2 and Fig. 2a), literally suggesting that the sorption mainly occurred *via* simple chemical reaction (Nethaji et al., 2013). Both the KOH and H_2O_2-treated SSD biochars showed faster removal kinetics than the raw biochar, reaching the equilibrium in less than 5 h for BH_2O_2 and BKOH, and after 10 h for BSS (Fig. 2a). These results are consistent with a previous study with faster kinetics on the KOH-modified switchgrass biochar than the raw biochar (Regmi et al., 2012). Fig. 2b shows that the plots did not pass through the origin as the C values are not equal to zero (Table 2). This indicates some degree of boundary layer and the intraparticle diffusion was not the only rate controlling step, but other mechanisms like film diffusion and external mass transfer may also play important roles in the sorption (Nethaji et al., 2013).

Sorption isotherms are shown in Fig. 3, and the corresponding parameters can be found in Table 3 and Table S3 (supplementary information). Cd sorption was better described by the

Langmuir model (Table S3), suggesting the possibility of a monolayer sorption of Cd onto the homogeneous biochar surfaces (Zhao et al., 2015b). The Langmuir maximal sorption capacity, Q_m, increased by a 15-fold to 20-fold factor after treatment with H_2O_2 and KOH, respectively (Table 3). This can be linked to the previous observation that the chemical treatments not only increase the S_{BET}, but also the CEC, resulting in an increase of the sorption sites and exchangeable cations. The higher Q_m value of BKOH compared to BH_2O_2 is consistent with the more pronounced improvement of both S_{BET} and CEC with the KOH treatment (Table 1).

The effect of the washing procedure applied after KOH treatment on the adsorption kinetics and isotherms are shown in Fig. 2 and 3 and Tables 2 and 3. The sorption kinetic constant for biochar with the KOH treatment was lower without the column washing step, but the value was still higher than that for the raw biochar. This finding could result from the reduction of S_{BET} for the insufficient batch washed $BKOH^{bat}$. A slightly higher Q_m was observed for $BKOH^{bat}$ compared to BKOH, meaning that the sorption of this cationic metal was not strongly affected by the washing procedure. The release of ions and organic compounds from the $BKOH^{bat}$ did not appear to modify the Cd(II) behavior, in contrast to what was observed in a previous study with Pb(II) (Wongrod et al., 2018). This could be due to a higher affinity of Cd(II) for biochar sites (*i.e.* higher K_L values than Pb(II)) and/or weaker interactions between Cd(II) and dissolved compounds in the solutions. For example in our findings, the K_L values of BKOH were 0.032 l μmol^{-1} and 0.007 l μmol^{-1} for Cd(II) and Pb(II), respectively (Wongrod et al., 2018).

3.3 Arsenic sorption

3.3.1 Effect of chemical treatment of biochar on As(V) sorption

Fig. 4(a) shows the effect of chemical treatments on the adsorption kinetics for As(V) onto BSS, BH_2O_2 and BKOH. All experimental data fitted with a pseudo-second-order kinetic model ($R^2 \geq 0.98$, Table S2, supplementary information) and corresponding parameters are given in Table 2. These results showed that the sorption kinetics were unchanged for BH_2O_2, with a sorption equilibrium reached after 10 h, while it was reached after 24 h for BKOH.

The sorption isotherms for As(V) are shown in Fig. 4(b). Similar to Cd, the Langmuir model provided the best fit for As(V) sorption (Table S3, supplementary information). The corresponding sorption parameters are given in Table 3. No significant evolution was observed for the values of K_L, indicating that the chemical treatments did not modify the affinity of the biochar for As(V). In contrast, the sorption capacity was enhanced by both H_2O_2 and KOH-treated biochars (except $BKOH^{bat}$), and the Q_m values being, respectively, about 4 times and 5 times higher than the raw biochar.

These results indicate that H_2O_2 treatment only improved the sorption capacity, whereas KOH treatment improved the sorption capacity but induced slower sorption kinetics for As(V) (Tables 2 and 3). In both cases, the enhanced sorption ability for As(V) by the chemically-modified biochars could be linked to the increase of the S_{BET}, which was slightly higher for BKOH than BH_2O_2 (Table 1). These results are in agreement with previous studies (Ding et al., 2016; Wu et al., 2017), who showed that the surface area plays an important role in the sorption of elements onto biochar. The slightly increased pH_{pzc} of BKOH (Table 1) may result in a little

increase of the positive charges at the surface of the biochar, and thus enhance the sorption ability for the anionic As(V).

3.3.2 Comparison of biochar washing

The effect of the washing procedure applied after KOH treatment on the adsorption kinetics and isotherms for arsenic are presented in Fig. 5(a-d). The corresponding sorption parameters are given in Tables 2 and 3. The experiments were performed for As(V) and As(III) to determine if the washing procedure affects similarly both arsenic species, taking into account that, in the experimental conditions, As(III) is neutral whereas As(V) is negatively-charged.

It appeared that the washing procedures of KOH-biochars had a low impact on the sorption kinetics for As(III), k_2 values increasing from 0.20 (± 0.05) h^{-1} to 0.38 (± 0.07) h^{-1} with the addition of the subsequent column washing step (Fig. 5a). In contrast, the addition of this step strongly affected the sorption kinetics for As(V) (Fig. 5b), inducing a 3-fold decrease of k_2 (Table 2). The sorption isotherms showed an opposite trend: the column washing step only marginally modified the Q_m of the biochar for As(III), but induced an almost 10-fold improvement for As(V). This strong difference of the Q_m values for As(V) can be attributed to the PO_4^{3-} released from $BKOH^{bat}$, as highlighted in a previous study (Wongrod et al., 2018). Indeed, the PO_4^{3-} may strongly compete with As(V) for sorption onto the biochar. It has been previously established that excessive PO_4^{3-} concentrations could mobilize As(V) from the sorbent (Neupane et al., 2014). This is likely due to the similar chemical properties between PO_4^{3-} and As(V) since both chemicals are negatively-charged oxyanions. Moreover, the leaching of dissolved organic carbon (DOC) from the biochar (Wongrod et al., 2018) could accelerate the mobilization of As, as observed in a previous study in a biochar-soil system (Kim et al., 2018). Concerning the sorption constant K_L, there was no significant difference ($P \leq 0.01$) according to the washing procedures for As(V) and As(III), indicating that no evolution in the affinity of biochar for both arsenic species was observed. When comparing K_L values between As(III) and As(V), it appears that the latter has less affinity for BKOH and $BKOH^{bat}$ (Table 3). It could be hypothesized from these results that arsenic species interact differently with the biochar surface or with different types of surface functions.

3.3.3 Evolution of arsenic redox speciation

The arsenic redox speciation in solution was determined during As(III) and As(V) sorption experiments in order to determine whether the biochar was able to induce redox conversions. During the sorption of As(III) onto $BKOH^{bat}$, up to 70% of arsenic in solution was As(V), despite only As(III) was initially added. A partial oxidation (<10%) was also observed in the presence of BKOH and no As(V) was detected in controls. In contrast, no reduction of As(V) to As(III) was noticed during As(V) sorption experiments. These results show that biochar is able to modify the arsenic redox state in solution and this could be strongly increased with an insufficient washing. These findings are in agreement with a previous study (Fakour and Lin, 2014) that reported an increased oxidation of As(III) in the presence of organic matter in solution.

4. Conclusions

Chemical treatment of biochar is considered to enhance the sorption performance for both oxyanions and cationic metals. The treatment with KOH or H_2O_2 strongly affects the sorption kinetics for As(III and V) and Cd(II). For As(V), KOH treatment induced a slower kinetic sorption compared to the raw biochar, while no significant variation was noticed for the H_2O_2-modified biochar. In contrast, both treatments showed faster sorption for Cd(II). All treatments induced a strong sorption capacity enhancement, particularly with alkali treatment. This is consistent with the observed evolutions of biochar properties such as CEC, S_{BET} and, to a lesser extent, pH_{ZPC}. Unfortunately, as previously highlighted, without the implementation of a careful washing procedure, this treatment also generated a strong release of inorganic and organic compounds from the biochar that can alter the evaluation of its sorption properties. This issue clearly affected As(V) sorption due to the competition with the released PO_4^{3-}.

When working with a redox-sensitive element, such as arsenic, it was observed that the biochar may also play an important role in the oxidation of As(III) to As(V). This phenomenon was enhanced by the insufficient washing process. The potential chemical transformation of arsenic should be carefully considered in future research in order to better understand the role of chemically-modified biochar on the removal of such compounds from contaminated water.

Acknowledgments

We thank Patrice Fondanèche (Université de Limoges, France) for technical assistance with the arsenic and cadmium analysis. This work was financially supported by the Marie Sklodowska-Curie European Joint Doctorate Advanced Biological Waste-to-Energy Technologies (ABWET) under the European Union's Horizon 2020 research and innovation programme (grant agreement N° 643071).

References

Agrafioti, E., Bouras, G., Kalderis, D., Diamadopoulos, E., 2013. Biochar production by sewage sludge pyrolysis. J. Anal. Appl. Pyrolysis 101, 72–78.

Ahmad, M., Rajapaksha, A.U., Lim, J.E., Zhang, M., Bolan, N., Mohan, D., Vithanage, M., Lee, S.S., Ok, Y.S., 2014. Biochar as a sorbent for contaminant management in soil and water: A review. Chemosphere 99, 19–23.

Aran, D., Maul, A., Masfaraud, J.F., 2008. A spectrophotometric measurement of soil cation exchange capacity based on cobaltihexamine chloride absorbance. Comptes. Rendus. Geosci. 340, 865–871.

Ding, Z., Hu, X., Wan, Y., Wang, S., Gao, B., 2016. Removal of lead, copper, cadmium, zinc, and nickel from aqueous solutions by alkali-modified biochar: Batch and column tests. J. Ind. Eng. Chem. 33, 239–245.

EPA, 1996. Method 3050B: Acid digestion of sediments, sludges, and soils. revision, 2, 1–12.

Fakour, H., Lin, T.F., 2014. Effect of humic acid on As redox transformation and kinetic adsorption onto iron oxide based adsorbent (IBA). Int. J. Environ. Res. Public Health 11, 10710–10736.

Gong, X.J., Li, W.G., Zhang, D.Y., Fan, W.B., Zhang, X.R., 2015. Adsorption of arsenic from micro-polluted water by an innovative coal-based mesoporous activated carbon in the presence of co-existing ions. Int. Biodeterior. Biodegrad. 102, 256–264.

Guo, K., Gao, B., Yue, Q., Xu, X., Li, R., Shen, X., 2018. Characterization and performance of a novel lignin-based flocculant for the treatment of dye wastewater. Int. Biodeterior. Biodegrad. 133, 99–107.

Ho, S.H., Chen, Y., Yang, Z., Nagarajan, D., Chang, J.S., Ren, N., 2017. High-efficiency removal of lead from wastewater by biochar derived from anaerobic digestion sludge. Bioresour. Technol. 246, 142–149.

Jiang, T., Xu, R., Gu, T., Jiang, J., 2014. Effect of crop-straw derived biochars on Pb(II) adsorption in two variable charge soils. J. Integr. Agric. 13, 507–516.

Kim, H. Bin, Kim, S.H., Jeon, E.K., Kim, D., Tsang, D.C.W., Alessi, D.S., Kwon, E.E., Baek, K., 2018. Effect of dissolved organic carbon from sludge, rice straw and spent coffee ground biochar on the mobility of arsenic in soil. Sci. Total Environ. 636, 1241–1248.

Li, H., Dong, X., da Silva, E.B., de Oliveira, L.M., Chen, Y., Ma, L.Q., 2017. Mechanisms of metal sorption by biochars: Biochar characteristics and modifications. Chemosphere 178, 466–478.

Liu, S., Huang, B., Chai, L., Liu, Y., Zeng, G., Wang, X., Zeng, W., Shang, M., Deng, J., Zhou, Z., 2017. Enhancement of As(V) adsorption from aqueous solution by a magnetic chitosan/biochar composite. RSC Adv. 7, 10891–10900.

Mahmood, T., Saddique, M.T., Naeem, A., Westerho, P., Mustafa, S., 2011. Comparison of different methods for the point of zero charge determination of NiO. Ind. Eng. Chem. Res. 50, 10017–10023.

Mohan, D., Sarswat, A., Ok, Y.S., Pittman, C.U., 2014. Organic and inorganic contaminants removal from water with biochar, a renewable, low cost and sustainable adsorbent – A critical review. Bioresour. Technol. 160, 191–202.

Nethaji, S., Sivasamy, A., Mandal, A.B., 2013. Adsorption isotherms, kinetics and mechanism for the adsorption of cationic and anionic dyes onto carbonaceous particles prepared from *Juglans regia* shell biomass. Int. J. Environ. Sci. Technol. 10, 231–242.

Neupane, G., Donahoe, R.J., Arai, Y., 2014. Kinetics of competitive adsorption/desorption of

arsenate and phosphate at the ferrihydrite-water interface. Chem. Geol. 368, 31–38.
Ofomaja, A.E., Pholosi, A., Naidoo, E.B., 2014. Kinetics and competitive modeling of cesium biosorption onto iron(III) hexacyanoferrate modified pine cone powder. Int. Biodeterior. Biodegrad. 92, 71–78.
Park, J.H., Wang, J.J., Kim, S.H., Cho, J.S., Kang, S.W., Delaune, R.D., Han, K.J., Seo, D.C., 2017. Recycling of rice straw through pyrolysis and its adsorption behaviors for Cu and Zn ions in aqueous solution. Colloids Surfaces A 533, 330–337.
Peng, Q., Zhang, F., Zhou, Y., Zhang, J., Wei, J., Mao, Q., Huang, H., Chen, A., Chai, L., Luo, L., 2018. Formation of composite sorbent by *P. chrysogenum* strain F1 and ferrihydrite in water for arsenic removal. Int. Biodeterior. Biodegrad. 132, 208–215.
Pituello, C., Francioso, O., Simonetti, G., Pisi, A., Torreggiani, A., Berti, A., Morari, F., 2014. Characterization of chemical–physical, structural and morphological properties of biochars from biowastes produced at different temperatures. J. Soils Sediments 15, 792–804.
Qiu, Y., Zheng, Z., Zhou, Z., Sheng, G.D., 2009. Effectiveness and mechanisms of dye adsorption on a straw-based biochar. Bioresour. Technol. 100, 5348–5351.
Rajapaksha, A.U., Chen, S.S., Tsang, D.C.W., Zhang, M., Vithanage, M., Mandal, S., Gao, B., Bolan, N.S., Ok, Y.S., 2016. Engineered/designer biochar for contaminant removal/immobilization from soil and water: Potential and implication of biochar modification. Chemosphere 148, 276–291.
Rajapaksha, A.U., Vithanage, M., Zhang, M., Ahmad, M., Mohan, D., Chang, S.X., Ok, Y.S., 2014. Pyrolysis condition affected sulfamethazine sorption by tea waste biochars. Bioresour. Technol. 166, 303–308.
Regmi, P., Garcia Moscoso, J.L., Kumar, S., Cao, X., Mao, J., Schafran, G., 2012. Removal of copper and cadmium from aqueous solution using switchgrass biochar produced via hydrothermal carbonization process. J. Environ. Manage. 109, 61–69.
Sizmur, T., Fresno, T., Akgül, G., Frost, H., Moreno-Jiménez, E., 2017. Biochar modification to enhance sorption of inorganics from water. Bioresour. Technol. 246, 34–47.
Wan, J., Pressigout, J., Simon, S., Deluchat, V., 2014. Distribution of As trapping along a ZVI/sand bed reactor. Chem. Eng. J. 246, 322–327.
Wang, C., Gu, L., Liu, X., Zhang, X., Cao, L., 2016. Sorption behavior of Cr(VI) on pineapple-peel-derived biochar and the influence of coexisting pyrene. Int. Biodeterior. Biodegradation 111, 78–84.
Wongrod, S., Simon, S., Guibaud, G., Lens, P.N.L., Pechaud, Y., Huguenot, D., van Hullebusch, E.D., 2018. Lead sorption by biochar produced from digestates: Consequences of chemical modification and washing. J. Environ. Manage. 219, 277–284.
Wu, W., Li, J., Lan, T., Müller, K., Khan, N., Chen, X., Xu, S., Zheng, L., Chu, Y., Li, J., Yuan, G., Wang, H., 2017. Unraveling sorption of lead in aqueous solutions by chemically modified biochar derived from coconut fiber: A microscopic and spectroscopic investigation. Sci. Total Environ. 576, 766–774.
Yuan, H., Lu, T., Huang, H., Zhao, D., Kobayashi, N., Chen, Y., 2015. Influence of pyrolysis temperature on physical and chemical properties of biochar made from sewage sludge. J. Anal. Appl. Pyrolysis 112, 284–289.
Zama, E.F., Zhu, Y.G., Reid, B.J., Sun, G.X., 2017. The role of biochar properties in influencing the sorption and desorption of Pb(II), Cd(II) and As(III) in aqueous solution. J. Clean. Prod. 148, 127–136.
Zhao, L., Xue, F., Yu, B., Xie, J., Zhang, X., Wu, R., Wang, R., Hu, Z., Yang, S.T., Luo, J., 2015a. TiO_2–graphene sponge for the removal of tetracycline. J. Nanoparticle Res. 17, 1–9.

Zhao, Z., Wu, M., Jiang, Q., Zhang, Y., Chang, X., Zhan, K., 2015b. Adsorption and desorption studies of anthocyanins from black peanut skins on macroporous resins. Int. J. Food Eng. 11, 841–849.

Zhou, Z., Liu, Y., Liu, S., Liu, H., Zeng, G., Tan, X., Yang, C., Ding, Y., Yan, Z., Cai, X., 2017. Sorption performance and mechanisms of arsenic(V) removal by magnetic gelatin-modified biochar. Chem. Eng. J. 314, 223–231.

Zielińska, A., Oleszczuk, P., 2015. The conversion of sewage sludge into biochar reduces polycyclic aromatic hydrocarbon content and ecotoxicity but increases trace metal content. Biomass Bioenergy 75, 235–244.

Zuo, W.Q., Chen, C., Cui, H.J., Fu, M.L., 2017. Enhanced removal of Cd(II) from aqueous solution using $CaCO_3$ nanoparticle modified sewage sludge biochar. RSC Adv. 7, 16238–16243.

451 **Figures**

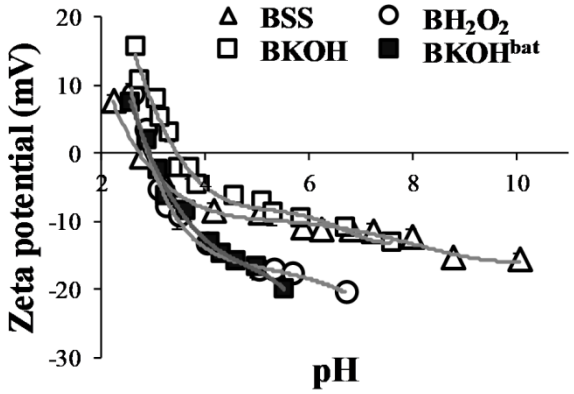

Fig. 1. Evolution of the zeta potential as a function of the pH values.

452

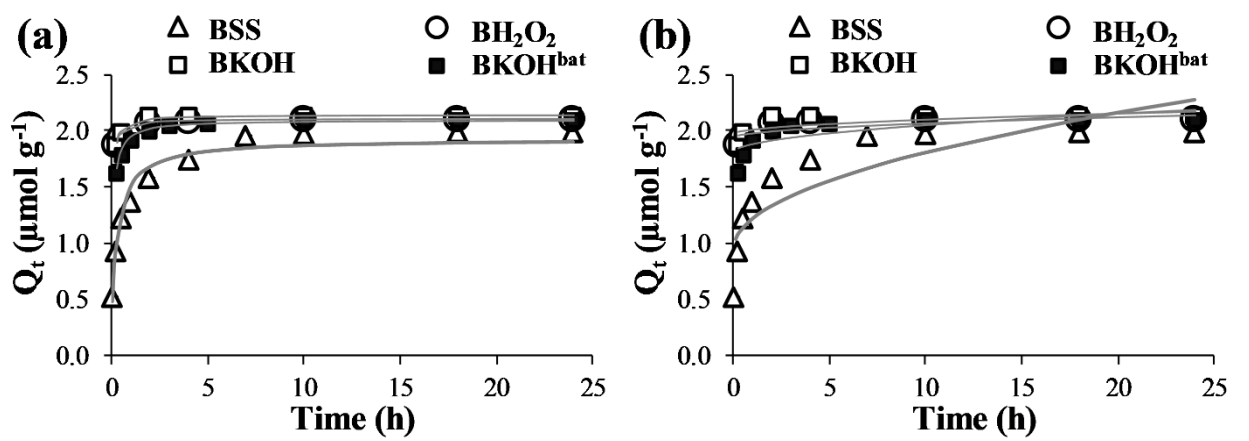

Fig. 2. Effect of chemical treatment and biochar washing on adsorption kinetics for Cd(II) by the raw and chemically-modified biochars fitted with the pseudo-second-order kinetic model (a), and with the intraparticle diffusion model (b) (initial pH=5, initial concentration: 10 µmol l^{-1}).

453

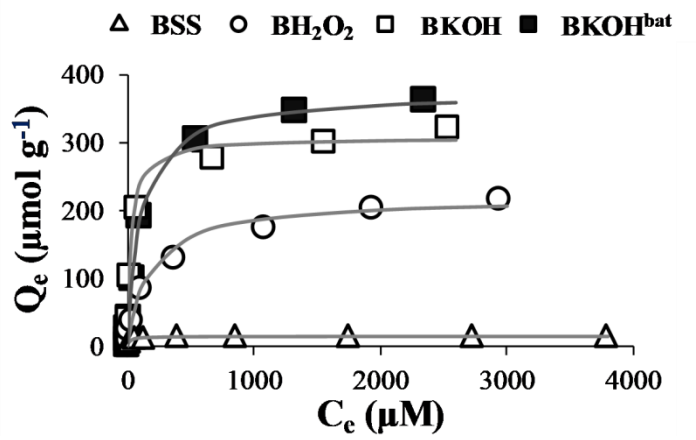

Fig. 3. Effect of chemical treatment and biochar washing on adsorption isotherms for Cd(II) by the raw and chemically-modified biochars (initial pH=5, 24 h, Langmuir model fitting).

454

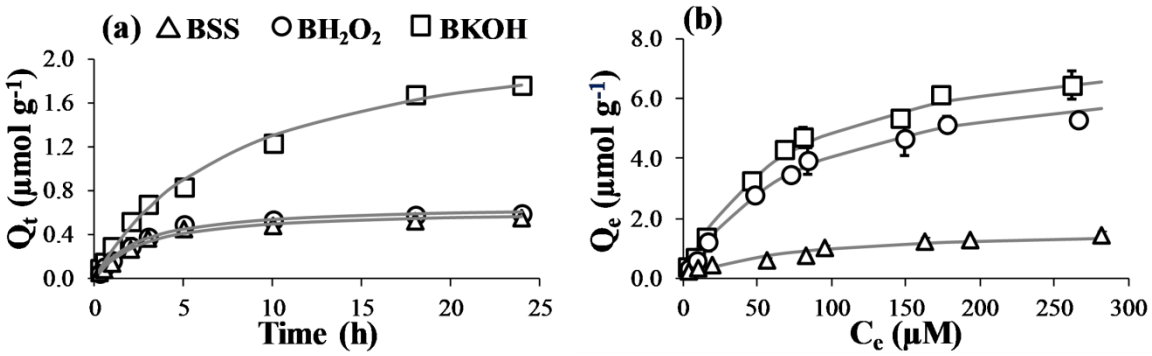

Fig. 4. Effect of chemical treatment on As(V) adsorption kinetics by biochars (a) (initial pH=5, initial concentration: 10 µmol l^{-1}, pseudo-second-order kinetic model fitting), and As(V) adsorption isotherms by biochars (b) (initial pH=5, 24 h, Langmuir model fitting).

455

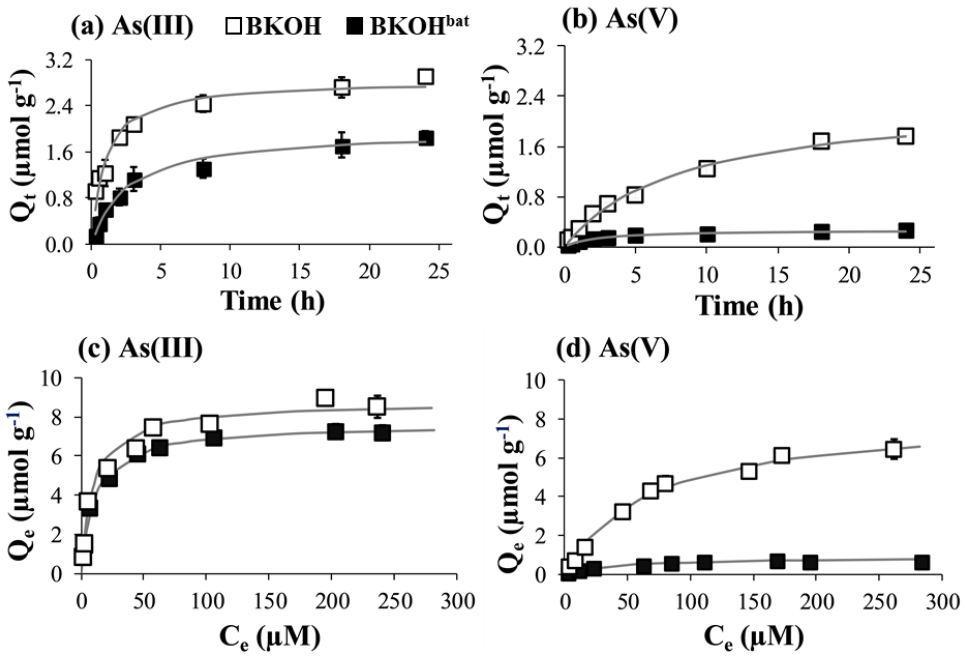

Fig. 5. Influence of biochar washing of KOH-modified biochars on adsorption kinetics for As(III) (a) and As(V) (b) (initial pH=5, initial concentration: 10 µmol l^{-1}, pseudo-second-order kinetic model fitting), and on adsorption isotherms for As(III) (c) and As(V) (d) (initial pH=5, 24 h, Langmuir model fitting).

456

Tables

Table 1. pH, electrical conductivity and surface area of the raw and chemically-modified biochars.

Biochar	pH in water	pH_{pzc}	Electrical conductivity (EC) ($\mu S\ cm^{-1}$)	S_{BET}[a] ($m^2\ g^{-1}$)	CEC[b] ($cmol^+\ kg^{-1}$)	Reference
BSS[c]	6.4 ±0.1	2.7	4.0 ±0.1	0.4 ±0.1	2.0 ±0.1	This study
BH_2O_2[c]	6.5 ±0.1	2.9	4.1 ±0.3	5.7 ±0.1	2.9 ±0.1	This study
BKOH[c]	8.4 ±0.1	3.4	6.2 ±0.5	7.9 ±0.1	13.4 ±0.1	This study
$BKOH^{bat}$ [c]	10.0 ±0.1	2.9	324.0 ±2.4	3.0 ±0.1	20.8 ±0.1	This study
Sewage sludge (300 °C)	6.7 ±0.2	na[d]	7750.0 ±160.0	14.3 ±0.2	na	Yuan et al. (2015)
Sewage sludge (300 °C)	na	na	na	4.0	na	Agrafioti et al. (2013)

[a] S_{BET} refers to Brunauer-Emmett-Teller surface area of biochar.

[b] CEC refers to cation exchange capacity of biochar.

[c] BSS: biochar from sewage sludge digestate, BH_2O_2: H_2O_2-modified biochar, BKOH and $BKOH^{bat}$: KOH-modified biochars, respectively, with batch and column washing, and with batch washing.

[d] na refers to not available.

Table 2. Constants for adsorption kinetics of As(III), As(V) and Cd(III) by biochars with the pseudo-second-order and intraparticle diffusion models.

Pseudo-second-order model

Biochar	As(III)			As(V)			Cd(II)		
	k_2[a]	Q_e[b]	R^2	k_2	Q_e	R^2	k_2	Q_e	R^2
BSS[c]	-	-	-	0.630 ±0.098	0.62 ±0.03	0.985	1.724 ±0.204	1.93 ±0.04	0.983
BH_2O_2[c]	-	-	-	0.619 ±0.092	0.66 ±0.03	0.985	12.251 ±0.803	2.09 ±0.01	9.985
BKOH[c]	0.378 ±0.067	2.83 ±0.11	0.961	0.052 ±0.006	2.35 ±0.09	0.995	12.907 ±0.479	2.14 ±0.01	0.993
BKOH[bat c]	0.205 ±0.042	1.94 ±0.10	0.975	1.599 ±0.340	0.27 ±0.02	0.969	6.298 ±0.338	2.09 ±0.10	0.987

Intraparticle diffusion model

Biochar	As(III)			As(V)			Cd(II)		
	k_i[d]	C	R^2	k_i	C	R^2	k_i	C	R^2
BSS	-	-	-	0.115 ±0.013	0.065 ±0.035	0.910	0.269 ±0.039	0.956 ±0.101	0.852
BH_2O_2	-	-	-	0.121 ±0.014	0.083 ±0.036	0.913	0.042 ±0.010	1.932 ±0.029	0.787
BKOH	0.429 ±0.044	0.981 ±0.113	0.938	0.396 ±0.012	-0.074 ±0.030	0.993	0.041 ±0.013	1.973 ±0.036	0.699
BKOH[bat]	0.358 ±0.033	0.219 ±0.086	0.948	0.050 ±0.006	0.036 ±0.015	0.919	0.077 ±0.018	1.799 ±0.046	0.749

[a] k_2 unit: g(μmol h)$^{-1}$.

[b] Q_e unit: in μmol g^{-1}.

[c] BSS: biochar from sewage sludge digestate, BH_2O_2: H_2O_2-modified biochar, BKOH and BKOH[bat]: KOH-modified biochars, respectively, with batch and column washing, and with batch washing.

[d] k_i unit: μmol (g h$^{1/2}$)$^{-1}$.

Table 3. Parameters determined from adsorption isotherms for As(III), As(V) and Cd(II) by biochars with the Langmuir model.

Biochar	As(III)			As(V)			Cd(II)		
	K_L[a]	Q_m[b]	R^2	K_L	Q_m	R^2	K_L	Q_m	R^2
BSS[c]	-	-	-	0.015 ±0.006	1.60 ±0.23	0.958	0.061 ±0.009	15.49 ±0.32	0.992
BH_2O_2[c]	-	-	-	0.012 ±0.003	7.22 ±0.67	0.989	0.005 ±0.001	218.73 ±6.91	0.990
BKOH[c]	0.103 ±0.018	8.74 ±0.33	0.976	0.014 ±0.003	8.11 ±0.53	0.994	0.032 ±0.004	306.09 ±6.07	0.994
$BKOH^{bat}$[c]	0.088 ±0.007	7.60 ±0.12	0.996	0.024 ±0.008	0.85 ±0.09	0.965	0.009 ±0.001	372.49 ±6.71	0.996

[a] K_L unit: in l μmol^{-1}.

[b] Q_m unit: in $\mu mol\ g^{-1}$.

[c] BSS: biochar from sewage sludge digestate, BH_2O_2: H_2O_2-modified biochar, BKOH and $BKOH^{bat}$: KOH-modified biochars, respectively, with batch and column washing, and with batch washing.

Supplementary Information

Changes of sewage sludge digestate-derived biochar properties after chemical treatments and the influence on As(III and V) and Cd(II) sorption

Suchanya Wongrod[a,b,c], Stéphane Simon[b,†], Eric D. van Hullebusch[a,c,d], Piet N.L. Lens[c], Gilles Guibaud[b]

[a] Université Paris-Est, Laboratoire Géomatériaux et Environnement (EA 4508), UPEM, 77454, Marne-la-Vallée, France

[b] Université de Limoges, PEIRENE, Equipe Développement d′indicateurs ou prévision de la qualité des eaux, URA IRSTEA, 123 avenue Albert Thomas, 87060 Limoges, France

[c] UNESCO-IHE Institute for Water Education, P.O. Box 3015, 2601 DA Delft, The Netherlands

[d] Institut de Physique du Globe de Paris, Sorbonne Paris Cité, Université Paris Diderot, UMR 7154, CNRS, F-75005 Paris, France

[†] Corresponding author. Université de Limoges, PEIRENE, Equipe Développement d′indicateurs ou prévision de la qualité des eaux, URA IRSTEA, 123 avenue Albert Thomas, 87060 Limoges, France
Email: stephane.simon@unilim.fr

Measurement of pH of point of zero charge (pH_{PZC}) of biochar

The pH_{PZC} of raw and chemically-modified biochars was determined from zetametry by determining the zeta potential at different pH ranges (Mahmood et al., 2011). Firstly, 40 mL of background electrolyte solution (0.01 M $NaNO_3$) containing 0.2 g of biochar was equilibrated with continuous magnetic stirring at 20 (± 2) °C for 40 min. The pH of the mixture was adjusted in the range of 2.0 – 10.0 by using HNO_3 (0.1, 0.5 and 1 M) and NaOH (0.1, 0.5 and 1 M). After 40 min of stirring, the pH was measured and readjusted to correct the pH value until each solution reached a stable pH. The suspension was then filtered with a 0.45 µm cellulose acetate syringe filter before determining the zeta potential (Zetasizier Nanoseries (Nano-ZS), Malvern, UK). This filtration was performed to prevent the settlement of biochar particles in the measurement cell of the zetameter and to avoid the clogging of big particles in the device. We hypothesize that all biochar particles display the same behavior, neglecting the particle size.

Measurement of the cation exchange capacity (CEC) of biochar

For the determination of the CEC, 2 g of biochar (dry weight) were mixed with 40 mL of 0.05 N **cobalt hexamine trichloride** ($[Co(NH_3)_6]Cl_3$) solution (99% w/w, Sigma-Aldrich) in polypropylene tubes (Aran et al., 2008). The suspensions were shaken for 1 h using an orbital shaker (KS 501 digital, IKA^{TM}, USA) at 60 rpm, then centrifuged at 7000 g for 10 min (Rotina 420, Hettich, Germany). The supernatant was filtered through Whatman polyethersulfone syringe filters (0.2 µm). The pH (Präzisions-pH-meter E510, Metrohm AG, Switzerland) and absorbency at 472 nm (UV–vis spectrophotometer, Lambda 365, PerkinElmer, USA) of each sample were measured immediately. All experiments were performed in triplicate and the results are reported as mean values. The CEC (meq 100 g^{-1} or $cmol^+$ kg^{-1}) can be calculated as follows using Eq. (1) (Aran et al., 2008):

$$CEC = \left[\frac{Abs_{Co} - Abs_{sample}}{Abs_{Co}}\right] \times 50 \times \frac{V}{m} \times 100 \quad (1),$$

where Abs_{Co} and Abs_{sample} refer to the absorbency (at 472 nm) of 0.05 N $[Co(NH_3)_6]Cl_3$ and of sample (supernatant after filtration), respectively. V and m correspond to solution volume in liter and biochar dry mass in gram, respectively.

X-ray powder diffraction (XRD) analysis

X-ray diffractometry (XRD) was employed to identify the crystalline structures presented in raw and modified biochars. The samples were grounded to less than 100 µm particle size and were characterized using a powder diffractometer (AXS D8, Bruker, Germany) with Cu Kα radiation at 1.54 Å wavelength over the 2θ range from 10° to 32°, for 10 seconds per step, at 40 kV voltage

and 40 mA current with a Solx (Si-Li) detector. The crystalline compounds present in biochar were identified using the X'Pert HighScore software for data analysis with the reference from the International Center for Diffraction Data (ICDD).

Fourier-transform infrared spectroscopy (FTIR) analysis

FTIR spectra were recorded to identify the functional groups present on biochar surfaces. Each sample was mixed with KBr in a ratio of 1 mg sample (particle size 100 µm) per 200 mg KBr and the pellet was prepared by compression under vacuum (Jouraiphy et al., 2005). The analysis was performed using a Shimadzu IRAffinity-1 Spectrometer with a deuterated-triglycine sulfate (DTGS) detector. The number of scans was 12 with a resolution of 16 cm-1 and a frequency in a range from 4000 to 800 cm-1.

555 **XRD spectra of raw sewage sludge digestate and its derived biochar**

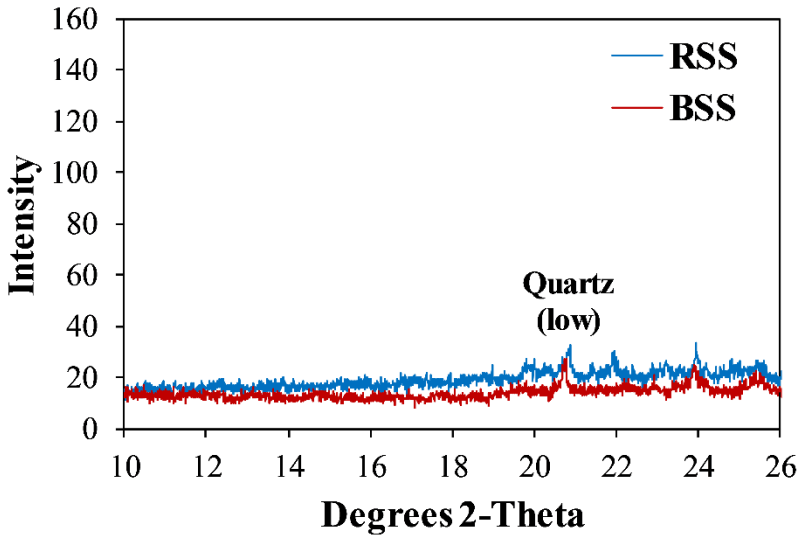

Fig. S1. XRD spectra of raw sewage sludge digestate (RSS) and biochar from sewage sludge digestate (BSS) produced at 350 °C under slow pyrolysis.

556

FTIR spectra of raw sewage sludge digestate and its derived biochar

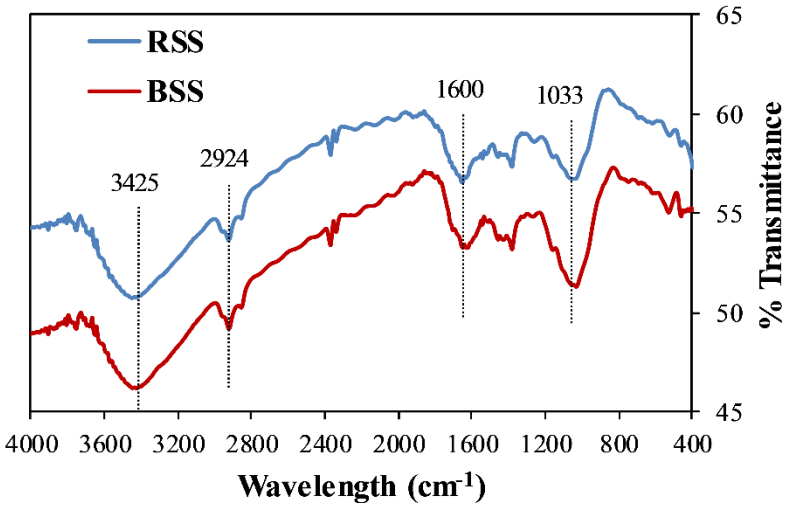

Fig. S2. FTIR spectra of raw sewage sludge digestate (RSS) and biochar from sewage sludge digestate (BSS) produced at 350 °C under slow pyrolysis.

559

560 **Table S1.** Comparison of the sorption performance of As(V) and Cd(II) by different types of biochars.

Adsorbent	Element	Maximum adsorption capacity (μmol g^{-1})	Concentration ranges (μM)	Solution pH	References
BSS[a]	As(V)	1.6	10 – 300	5.0	This study
BH_2O_2[a]	As(V)	7.1	10 – 300	5.0	This study
BKOH[a]	As(V)	8.5	10 – 300	5.0	This study
Fe(II)-loaded activated carbon	As(V)	27	7 – 113	3.0	Özge et al. (2013)
Paper mill sludge biochar	As(V)	303	280 – 2529	6.5	Yoon et al. (2017)
Magnetic carbonaceous tea waste	As(V)	507	10 – 1335	5.0	Wen et al. (2017)
Carbonaceous nanofibers	As(V)	670	100 – 900	5.0	Cheng et al. (2016)
BSS	Cd(II)	16	10 – 4000	5.0	This study
BH_2O_2	Cd(II)	220	10 – 4000	5.0	This study
BKOH	Cd(II)	318	10 – 4000	5.0	This study
Paper mill sludge biochar	Cd(II)	369	187 – 2506	6.5	Yoon et al. (2017)
H_2O_2-treated yak manure biochar	Cd(II)	419	10 – 1779	-	Wang and Liu (2018)
Graphene oxide nanosheets	Cd(II)	945	40 – 450	6.0	Zhao et al. (2011)

561 [a] BSS, BH_2O_2 and BKOH refer to, respectively, biochar produced from sewage sludge digestate, and its derived biochar with H_2O_2 and
562 KOH treatments.

563 **Table S2.** Chemical characteristics of raw sewage sludge digestate (RSS) and its derived biochar
564 produced at 350 °C under slow pyrolysis (BSS).

Parameters	RSS	BSS
pH in water	6.0 ±0.1	6.4 ±0.1
As (mg kg^{-1})	79 ±3[a]	47 ±1
Cd (mg kg^{-1})	dl[b]	9 ±1
Cr (mg kg^{-1})	42 ±1	48 ±1
Cu (mg kg^{-1})	390 ±10	617 ±7
Ni (mg kg^{-1})	25 ±1	41 ±1
Pb (mg kg^{-1})	80 ±9	85 ±3
Zn (mg kg^{-1})	756 ±10	1017 ±13

565 [a] Values reported as means (n=3) on dry mass basis followed by standard deviation.

566 [b] dl refers to value below detection limit.

Adsorption kinetics

The sorption kinetic data for arsenic and cadmium by biochars was calculated using the pseudo-first-order (PFO) (Eq. 2), pseudo-second-order (PSO) (Eq. 3) and intraparticle diffusion (Eq. 4) kinetic models, which are illustrated as followed:

$$\log(Q_e - Q_t) = \log Q_e - \frac{k_1 t}{2.303} \quad (2),$$

$$\frac{t}{Q_t} = \frac{1}{k_2 Q_e^2} + \frac{t}{Q_e} \quad (3),$$

$$Q_t = k_i t^{1/2} + C \quad (4),$$

where Q_t and Q_e are arsenic or cadmium adsorption capacity (μmol g^{-1}) at time t (h) and at equilibrium, k_1 (h^{-1}), k_2 ($g(\mu mol\ h)^{-1}$) and k_i ($\mu mol\ (g\ h^{1/2})^{-1}$) are the rate constants for the PFO, PSO and intraparticle diffusion kinetic models, respectively (Liu and Zhang, 2009; Zhao et al., 2015). C is the intraparticle diffusion constant related to the boundary layer diffusion. All uncertainties of sorption kinetic parameters were obtained by non-linear regression using Statistica software (v6.1, StatSoft).

Adsorption isotherms

Langmuir and Freundlich models are presented, respectively, in Eqs. (4) and (5):

$$\frac{C_e}{Q_e} = \frac{1}{K_L Q_m} + \frac{C_e}{Q_m} \quad (5),$$

$$\ln Q_e = \ln K_F + \frac{1}{n} \ln C_e \quad (6),$$

where C_e is the equilibrium arsenic or cadmium solution concentration (μM). Q_e and Q_m are the arsenic or cadmium adsorption capacity at equilibrium and at maximum capacity (μmol g^{-1}), respectively. K_L and K_F are the adsorption constants for the Langmuir and Freundlich isotherm models, and n is the Freundlich constant which indicates the favorability of adsorption, respectively.

590 **Table S3.** Constants for the pseudo-first-order (PFO), pseudo-second-order (PSO) and intraparticle diffusion kinetic models for As(III,
591 V) and Cd(II) sorption by different types of biochars (BSS: biochar from sewage sludge digestate, BH_2O_2: H_2O_2-modified biochar, BKOH and
592 $BKOH^{bat}$: KOH-modified biochars, respectively, with batch and column washing and with batch washing).

Biochar	As(III)								
	PFO			PSO			Intraparticle diffusion		
	k_1 [a]	Q_e [b]	R^2	k_2 [a]	Q_e	R^2	k_i	C	R^2
BSS	-	-	-	-	-	-	-	-	-
BH_2O_2	-	-	-	-	-	-	-	-	-
BKOH	0.128	1.62	0.934	0.378	2.83	0.961	0.429	0.981	0.938
$BKOH^{bat}$	0.134	1.44	0.967	0.205	1.94	0.975	0.358	0.219	0.948
Biochar	As(V)								
	PFO			PSO			Intraparticle diffusion		
	k_1	Q_e	R^2	k_2	Q_e	R^2	k_i	C	R^2
BSS	0.167	0.40	0.918	0.630	0.62	0.985	0.115	0.065	0.910
BH_2O_2	0.188	0.44	0.948	0.619	0.66	0.985	0.121	0.083	0.913
BKOH	0.165	1.84	0.969	0.052	2.35	0.995	0.396	-0.074	0.993
$BKOH^{bat}$	0.139	0.19	0.954	1.599	0.27	0.969	0.050	0.036	0.919
Biochar	Cd(II)								
	PFO			PSO			Intraparticle diffusion		
	k_1	Q_e	R^2	k_2	Q_e	R^2	k_i	C	R^2
BSS	0.184	0.94	0.923	1.724	1.93	0.983	0.269	0.956	0.852
BH_2O_2	0.400	0.14	0.881	12.251	2.09	9.985	0.042	1.932	0.787
BKOH	1.217	0.19	0.763	12.907	2.14	0.993	0.041	1.973	0.699
$BKOH^{bat}$	0.652	0.38	0.942	6.298	2.09	0.987	0.077	1.799	0.749

593 [a] k_1 and k_2 units: h^{-1} and $g(\mu mol\ h)^{-1}$, respectively.

594 [b] Q_e unit: in $\mu mol\ g^{-1}$.

Table S4. Constants for the Langmuir and Freundlich isotherms for As(III), As(V) and Cd(II) sorption by different types of biochars (BSS: biochar from sewage sludge digestate, BH_2O_2: H_2O_2-modified biochar, BKOH and $BKOH^{bat}$: KOH-modified biochars, respectively, with batch and column washing and with batch washing).

Biochar	As(III)						As(V)						Cd(II)					
	Langmuir			Freundlich			Langmuir			Freundlich			Langmuir			Freundlich		
	K_L[a]	Q_m[b]	R^2	K_F[c]	n	R^2	K_L	Q_m	R^2	K_F	n	R^2	K_L	Q_m	R^2	K_F	n	R^2
BSS	-	-	-	-	-	-	0.015	1.60	0.958	0.112	2.185	0.986	0.061	15.49	0.992	3.163	4.336	0.796
BH_2O_2	-	-	-	-	-	-	0.012	7.22	0.989	0.156	1.456	0.966	0.005	218.73	0.990	5.893	2.008	0.942
BKOH	0.103	8.74	0.976	1.059	2.299	0.884	0.014	8.11	0.994	0.196	1.473	0.967	0.032	306.09	0.994	23.460	2.570	0.933
$BKOH^{bat}$	0.088	7.60	0.996	1.007	2.420	0.880	0.024	0.85	0.965	0.044	1.867	0.906	0.009	372.49	0.996	9.013	1.849	0.882

[a] K_L unit: in l μmol^{-1}.

[b] Q_m unit: in $\mu mol\ g^{-1}$.

[c] K_F unit: in $(\mu mol\ g^{-1})(l\ \mu mol^{-1})^{1/n}$.

References

Aran, D., Maul, A., Masfaraud, J.F., 2008. A spectrophotometric measurement of soil cation exchange capacity based on cobaltihexamine chloride absorbance. Comptes. Rendus. Geosci. 340, 865–871.

Cheng, W., Ding, C., Wang, X., Wu, Z., Sun, Y., Yu, S., Hayat, T., Wang, X., 2016. Competitive sorption of As(V) and Cr(VI) on carbonaceous nanofibers. Chem. Eng. J. 293, 311–318.

Jouraiphy, A., Amir, S., El Gharous, M., Revel, J.C., Hafidi, M., 2005. Chemical and spectroscopic analysis of organic matter transformation during composting of sewage sludge and green plant waste. Int. Biodeterior. Biodegrad. 56, 101–108.

Liu, Z., Zhang, F.S., 2009. Removal of lead from water using biochars prepared from hydrothermal liquefaction of biomass. J. Hazard. Mater. 167, 933–939.

Mahmood, T., Saddique, M.T., Naeem, A., Westerho, P., Mustafa, S., 2011. Comparison of different methods for the point of zero charge determination of NiO. Ind. Eng. Chem. Res. 50, 10017–10023.

Tuna, A.O.A., Ozdemir, E., Simsek, E.B., Beker, U., 2013. Removal of As(V) from aqueous solution by activated carbon-based hybrid adsorbents: Impact of experimental conditions. Chem. Eng. J. 223, 116–128.

Wang, Y., Liu, R., 2018. H_2O_2 treatment enhanced the heavy metals removal by manure biochar in aqueous solutions. Sci. Total Environ. 628–629, 1139–1148.

Wen, T., Wang, J., Yu, S., Chen, Z.S., 2017. Magnetic porous carbonaceous material produced from tea waste for efficient removal of As(V), Cr(VI), humic acid and dyes. ACS Sustain. Chem. Eng. 5, 4371–4380.

Yoon, K., Cho, D.W., Tsang, D.C.W., Bolan, N., Rinklebe, J., Song, H., 2017. Fabrication of engineered biochar from paper mill sludge and its application into removal of arsenic and cadmium in acidic water. Bioresour. Technol. 246, 69–75.

Zhao, G., Li, J., Ren, X., Chen, C., Wang, X., 2011. Few-layered graphene oxide nanosheets as superior sorbents for heavy metal ion pollution management. Environ. Sci. Technol. 45, 10454–10462.

Zhao, Z., Wu, M., Jiang, Q., Zhang, Y., Chang, X., Zhan, K., 2015. Adsorption and desorption studies of anthocyanins from black peanut skins on macroporous resins. Int. J. Food Eng. 11, 841–849.